

Boundary Helps: Efficient Routing Protocol using Directional Antennas in Cognitive Radio Networks

Ying Dai and Jie Wu

Department of Computer and Information Sciences
Temple University, Philadelphia, PA 19122
Email: {ying.dai, jiewu}@temple.edu

Abstract—The unpredictable activities of primary users (PUs) make the channel availabilities in cognitive radio networks (CRNs) very unstable. The dynamic channel availabilities cause routing in CRNs to be more difficult than in traditional wireless networks. Specifically, when a source node needs to select a route to reach the destination, the “optimal” route during the route selection phase may not be reliable because of the sudden appearance of a PU, and thus, may not be optimal during the data transmission phase. In this paper, we propose a novel routing protocol based on the source routing in traditional wireless networks. We consider the angle dimension of CRNs by assuming that the directional antennas are equipped on every node. The directional antennas can facilitate the marking of boundary areas of PUs. We use the USRP/Gnuradio to show the sensing result differences of different directions at the boundary area of a primary user. For every optional route between a source node and a destination node, we can evaluate its reliability and other performance by evaluating the PU areas it passes through, and estimating the possible transmission rate of each link on this route. Based on these parameters, we propose an algorithm for route selection, considering both the reliability and delay. Our routing protocol only requires very limited piggyback information, compared to other routing protocols in CRNs. It is efficient and highly adaptable under the dynamic channel availabilities. We evaluate our approach through extensive simulations.

Index Terms—Cognitive radio networks, directional antennas, USRP/Gnuradio, boundary nodes, routing.

I. INTRODUCTION

Nodes, referred to as secondary users (SUs), in *cognitive radio networks* (CRNs) [1] can make opportunistic use of multiple channels not occupied by primary users (PUs). However, when a primary user becomes active and occupies a channel, SUs on that channel need to quit immediately. Therefore, some links can possibly be broken. The dynamics of channel availabilities result in the difficulty of routing in CRNs, and in carrying out end-to-end data transmission.

There have been many works on routing in CRNs [2]. Since the dynamic channel availabilities affect the delay and reliability of each route, the route selection algorithm needs to consider the channel availability situation of each optional route. A simple solution would be that each node collects its own information about PUs, and piggybacks that information to the source node for route selection. However, it will cause a lot of information exchange and burden the control channels.

Most of the existing routing protocols rely on the piggybacked channel information, and build their metrics regarding multiple parameters, e.g., channel availability and

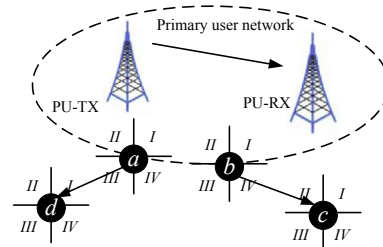


Fig. 1. Advantages of directional antenna in CRNs.

route quality. Then the route selection is usually based on these metrics. However, there are two main problems with these protocols. First, the overhead of the piggybacked information is usually too large, which makes it impractical when considering the energy and interference. Second, the piggybacked channel availabilities cannot convey the instant channel situation because, at the time the data is transmitting, the channel availabilities are possibly different. Therefore, a better protocol should be able to take both the overhead and dynamics in channel availabilities into consideration.

We consider the routing problem in a novel way, and make use of the directional antennas to help route selection. There have been many works done using directional antennas to benefit the data transmission in traditional wireless ad hoc networks [3]. There are two benefits to applying directional antennas. One is the reduction of radio interference. Thus, in CRNs, it increases the spacial reuse opportunities among PUs and SUs, and also for SUs themselves. Another benefit of directional antennas lies in the determination of if a node is located at the boundary of a PU area. For example, in Fig. 1, nodes *a* and *b* locate at the boundary of a PU network. Each node has a four-directional antenna. The four directions of the antenna on each node do not need to be globally aligned, which is similar to the directional antenna model in [4]. Although the pair of *PU-TX* and *PU-RX* is active, *a* and *b* can still use the same channel to send data in sector *III* and sector *IV*, respectively. In addition, the link from *a* to *d* and the link from *b* to *c* can use the same channel, since the directional transmission reduces the interference between them. We take both advantages of directional antennas in our model, and propose both a novel and efficient protocol.

In our paper, we assume that each node is equipped with a directional antenna, which is a reasonable assumption, considering the directional functions in many mobile devices

today. We define the boundary node, and each node is able to decide whether it is, itself, a boundary node or not. We use the USRP/Gnuadio testbed to show the difference among sensing results in different sectors of the directional antenna on a boundary node. We make use of the piggybacked information by boundary nodes. Here, instead of having every node along the route piggyback channel availability-related information, we only need the boundary node to piggyback that information. Therefore, our model induces less overhead during the piggyback phase, and also reduces the burden of information exchange on control channels. The source node makes use of the information returned by boundary nodes along each possible route, measures the channel availability and stability of each route, and chooses the best one to reach the destination node through our algorithm.

The main contributions of our work are as follows:

- We use the USRP/Gnuradio testbed to prove the sensing result differences of different directions of a boundary node, which provides the basis for a node to identify if itself is a boundary node.
- We make use of boundary nodes to piggyback information, with very limited overhead. The boundary nodes decide on the content of the information to piggyback, which is based on the threshold of PU activities.
- We redefine the route length in a creative way, which considers the channel availability, route stability, and the delay. Based on our defined route length, we give the algorithm for the route selection.

The organization of our paper is as follows. In Section II, we discuss the related works; we introduce two preliminaries in Section III; the problem is defined in Section IV; our routing protocol is described in Section V; performance evaluations are presented in Section VI; the conclusion is in Section VII.

II. RELATED WORKS

Our related works can be organized into two categories. One is about the routing protocols, and the other is about the existing directional antenna models in CRNs.

Many works have been done on routing protocols in CRNs. Most of them consider both routing and channel assignment. In [5], the authors propose a protocol called, opportunistic cognitive routing (OCR), which enables each user to make use of its geographical information and collect channel usage statistics. Then, OCR applies this information to perform routing and channel assignment. In [6], the authors study a routing protocol called CRP, which maps the spectrum selection metrics and local PU interference observations to a packet forwarding delay over the control channel. [7] develops a centralized channel assignment scheme and bandwidth allocation, combined with routing algorithms for multi-channel wireless mesh networks. Each node in their model is equipped with multiple network interface cards. [8] presents a routing and channel assignment protocol for multi-channel multi-hop wireless networks. It balances channels by having each node select channels based on its load information. In [9], the authors consider a distributed channel assignment and

routing scheme in multi-channel multi-hop wireless networks. The channel cost metric (CCM) is introduced, which reflects the interference cost, and is defined as the sum of expected transmission times. Our work is different from the above protocols, since our model makes use of directional antennas, and only causes very limited overhead while considering the dynamic channel availabilities.

There are also some works done to take the angle dimension of CRNs into consideration. In [10], the authors propose a scheme with relays or directional relays for SUs to exploit new spectrum opportunities, and provide higher spectrum efficiency by coexistence of primary and CR users at the same region, time, and spectrum band. Particularly, they consider applying relay nodes when an existing link is broken. However, their solution is not very practical, since it assumes the known location information of different nodes, and does not consider the interference, the delay, or the power of each relay node. In [11], the authors use an electronically steerable parasitic antenna receptor to study the spectrum sensing for cognitive radio. They divide the angular domain into sectors, and detect signals from PUs on a time domain. In [12], multicast communications in CRNs using directional antennas are studied. The authors control the transmission power to avoid interference with the PU network, and present a mathematical model, which is subsequently formulated as a Mixed Integer Non-linear Programming (MINLP) problem. In [13], the joint optimization of antenna orientation and spectrum allocation is studied. Their objective is to maximize the overall throughput of a CRN. Their model relies on the base station, and proposes a mathematical model, which is formulated as a MINLP; this is solved by adopting the branch and bound algorithm. The assumption of having known channel and node information is unrealistic. Moreover, their model is based on the base station, which takes no consideration of the multihop situation. Our model is different from the above ones, since we make use of the directional antenna to solve the routing problem. Also, our protocol is more efficient and practical.

III. PRELIMINARIES

In this section, we review two concepts. One is about the SINR model and the relation between transmission power and data transmission rate. The other is about the delay composition in CRNs.

A. Transmission Power and Rate

Suppose a node a sends data to node b using power P_a . The value of SINR [14] at b is:

$$SINR_{ab} = \frac{P_a g_{ab}}{N_0 + I},$$

where g_{ab} is the power gain from a to b , N_0 is the noise level, and I is the current interference by other nodes working on the same channel.

The maximum achievable data transmission rate V_{ab} of a given channel at b can then be computed based on Shannon's capacity theorem:

$$V_{ab} = W \log_2(1 + SINR_{ab}),$$

where W is the carrier bandwidth. Therefore, the more power that a can use to send would result in a better transmission rate on the link from a to b . We will discuss the constraints on P_a in the following section.

B. Delay Components

The delay of a routing path in CRNs is different from that in traditional wireless networks, due to the dynamic channel availability on each node. The main factors that influence the delay are:

- Medium access delay, which is the delay when a node accesses a given channel;
- Queuing delay, which is related to the output transmission rate of a node on a given channel;
- Handoff delay, which happens when the current channel is occupied by PUs, and the nodes need to switch to another channel;
- Rerouting delay, which is when the current link is unable to meet the transmission requirements, and the sender needs to seek another route to reach the receiver.

Therefore, if a routing path consists of many unstable links that need to be frequently handed off or rerouted, the overall delay would increase because of the increment in medium access delay, handoff delay, and rerouting delay. If the sender of a given link can only use low power to send, due to the interference requirements of PUs, this would result in low transmission rate, and the queuing delay would increase.

IV. PROBLEM FORMULATION

We first describe the system model and related constraints. Then, we give the objective of our model.

A. System Model & Constraints

We consider a CRN with the node set, $\{a, b, c, \dots\}$. Each node is equipped with directional antennas, which divides the omnidirectional transmission range of each node into a number of sectors. The total available channel set consists of M channels, which are licensed to a set of PUs, whose activities are unknown. During the data transmission, each node selects one sector to send the data. We assume that there is a common control channel (CCC) for nodes to coordinate.

There are several constraints that need to be satisfied for successful data transmission, regardless of which sector is adopted by each user. When node a sends data to node b , they must tune in to the same channel, $m \in M$. Suppose the power used by node a is P_a . The minimum SINR requirement at b is α_b . Therefore, we have

$$\frac{P_a g_{ab}}{N_0 + I} > \alpha_b. \quad (1)$$

Moreover, suppose that the nearby primary user pairs, $PU - TX$ and $PU - RX$, are working on the same channel m . Then, we have

$$\frac{P_p g_{pp}}{N_0 + I + g_{ap} P_a} > \alpha_p, \quad (2)$$

where P_p is the power adopted by $PU - TX$, g_{pp} is the power gain from $PU - TX$ to $PU - RX$, g_{ap} is the power gain

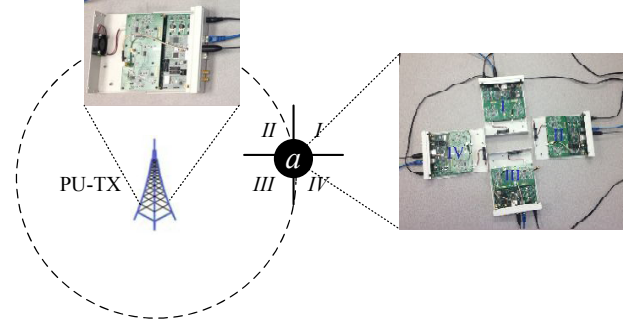


Fig. 2. Testbed for showing the characteristic of a boundary node.

from node a to $PU - RX$, and α_p denotes the desired SINR requirement of $PU - RX$. The data transmission from a to b is successful only if the above two constraints are satisfied.

Since the position of any $PU - TX$ is unknown to SUs, to make sure the PU sessions are not interfered with, we strengthen Constraint (2) as for any point within $PU - TX$'s area, instead of only $PU - RX$, where the SINR value is above α_p ; P_a must satisfy Constraint (2), no matter which sector a uses. Therefore, when a and $PU - TX$ are working on the same channel, we have the following three situations regarding the constraint of P_a , based on the distance between $PU - TX$ to node a :

$$P_a = \begin{cases} 0 & \frac{P_p g_{pa}}{N_0 + I} > \alpha_p, \\ P'_a & \frac{P_p g_{pp'}}{N_0 + I} = \alpha_p, g_{ap'} P'_a \rightarrow 0, \\ P_{max} & \frac{P_p g_{pp'}}{N_0 + I} = \alpha_p, g_{ap'} P_{max} = 0. \end{cases} \quad (3)$$

The first case is that when the SINR value of $PU - TX$ at a 's location is above α_p , a cannot use the channel of $PU - TX$. The second case is that a can use the channel of $PU - TX$, but the interference caused by a cannot make any point that has a SINR greater than or equal to α_p as being less than α_p . p' is a boundary point of $PU - TX$'s transmission area, where the SINR is equal to α_p . The third case is that a is far from $PU - TX$'s transmission area. Node a can transmit at the maximal power P_{max} without causing any significant interference to any point within $PU - TX$'s transmission area.

B. Objective

Suppose there are session requests in the CRN. For a source node S , the objective of our model is to find the route with the minimal delay while ensuring the reliability, as to reach the destination node, D . Based on the delay discussion in Section III, the channel availabilities on each link play an important factor in determining the overall delay. Since the channel availabilities on each link are dynamic, it is impractical to find the optimal solution. Even if a route provides the minimal delay at a given time, it is unable to ensure the minimal delay during the entire session.

We provide a protocol for routing which considers both delay and reliability, with the help of directional antennas. In our model, to select a route, there are four factors that need to be taken into consideration: the nodes on the route, the sector adopted by each node to transmit, the channel used on that

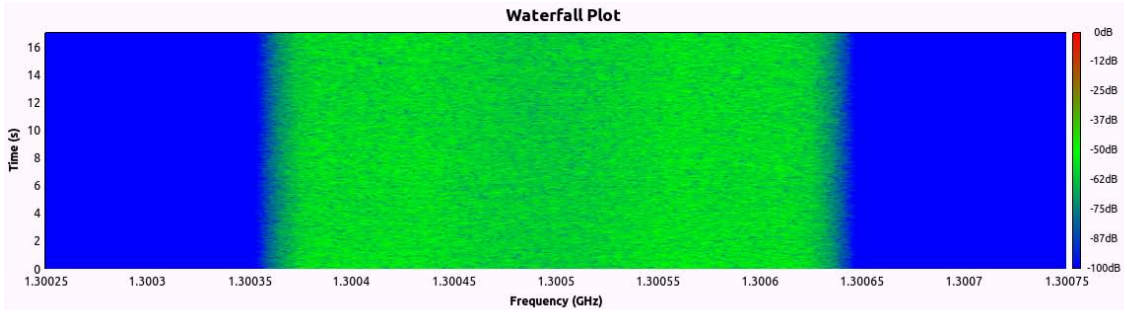


Fig. 3. Receiving results at sector I.

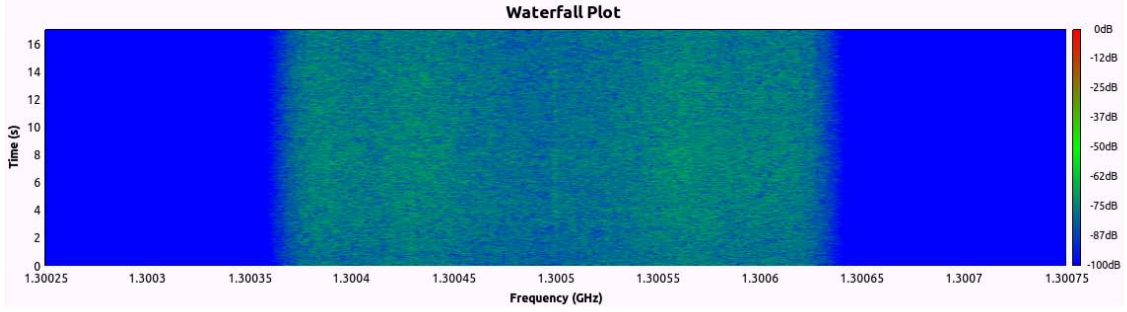


Fig. 4. Receiving results at sector II.

sector, and the power allowed on that channel. Considering the interference constraints of PUs and SUs are both dynamic, it is impractical to find the optimal solution. We propose an effective routing protocol, which makes use of the directional antennas, and efficiently reduces the overhead during the exchange of control messages on CCC. Our framework consists of two phases: route selection and data transmission.

V. ROUTING PROTOCOL WITH DIRECTIONAL ANTENNAS

A. Overview

Since each node in our model is equipped with a directional antenna, for a node a , we use the 2-tuple (IN_a, OUT_a) where IN_a denotes the sector ID that a packet is received by a , and OUT_a denotes the sector ID that the packet is sent out by a .

Similar to the source routing in traditional ad hoc networks [15], in our model, the source node first needs to find the route to reach the destination node using the following process:

- The source node, S sends the route request (RREQ) packet through the CCC from all sectors. The RREQ contains the ID of the destination node D , denoted as $\langle S, D \rangle$. Also, for every sector that the RREQ is sent out, it also contains the OUT_S . Since it is the source node, the IN_S is empty.
- For any node a that receives the RREQ, it would add its own node ID and broadcast the request through all of its sectors. Moreover, it would also add (IN_a, OUT_a) to the RREQ. Obviously, IN_a is the same for all sectors, from which the RREQ is received. OUT_a is different among the sending out of RREQ from different sectors.
- The above two processes continue until the destination node is reached. Then the RREQ will contain all the node IDs from S to D , denoted as $\langle S, \dots, a, \dots, D \rangle$. The RREQ also contains the IN and OUT sector IDs of each

node on the path, for example, the (IN_a, OUT_a) of node a . In addition, for destination node D , it only contains IN_D , since the OUT_D is empty.

After the destination node D is reached, it will reply with the route reply (RREP) packet over CCC, along with the route information (node IDs and sector numbers) in the RREQ packet, to the source node. Since, in most cases, there are several routes from S to D , the source node S needs to select one of them. It is intuitive to consider adding the channel availability situation of the corresponding sector on each node to the RREP message along the route, and piggybacking it to S . However, this is impractical. Since the channel availabilities on each sector of each node are dynamic, the channel availability of each node can be different between the piggyback phase and the data transmission phase. Also, it would cause lots of overhead to return the channel availability of every node on the route. In our model, we make use of the directional antennas, and propose an efficient route selection scheme.

B. Boundary Node

We first give the definition of *boundary node* under our model.

Definition 1: Node a is a boundary node regarding the $PU-TX$ on channel m if the variance, $V_a(m)$, of the sensing results in all sectors of node a is above a threshold, ν . We use $B_a(m) = 1$ to denote that c is the boundary node of $PU-TX$ that occupies channel m . Then

$$B_a(m) = \begin{cases} 0 & V_a(m) \leq \nu, \\ 1 & V_a(m) > \nu. \end{cases} \quad (4)$$

For example, in Fig. 5, $PU-TX$ occupies channel m_1 . $B_c(m_1) = 1$ if the variance of the sensing results on m in the

four sectors (I, II, III, IV) is above the threshold ν . It means that c is a boundary node of the $PU - TX$ that occupies channel m_1 .

We use the USRP/Gnuradio testbed to show the difference of the received SINR at different sectors of a boundary node. As shown in Fig. 2, to simulate a SU with a four-directional antenna, we use four USRP N200s, and each of them denotes one sector. Another USRP N200 is used to simulate a $PU - TX$. We use narrowband communication here. The PU sends on the channel with central frequency 1.3005GHz, and all the other 4 USRP N200s receive at the same channel. The received SINRs at the USRP N200s located at sectors I and II are shown in Figs. 3 and 4. We use the waterfall plot to show the SINR values over time. The approximate SINR at sector I is about -50 dB, while the value at sector II is about -87 dB. The differences of SINR values over time at different sectors of a boundary node are very obvious.

Besides, each boundary node records the historical probability, which is the probability of its corresponding PU to be active in a constant time range. For example, in Fig. 5, node c is a boundary node with $B_c(m_1) = 1$. It will maintain the active probability $PB_c(m_1)$ of $PU - TX$ in time range T . The value of $PB_c(m_1)$ is updated by node c after every T . We will use the $PB_c(m_1)$ in our piggyback scheme.

Many merits of boundary nodes have been studied in traditional wireless networks [16], [17]. In addition, boundary nodes in CRNs can facilitate the routing path selection. They can help to differentiate the routes that go into or avoid the $PU - TX$'s area. For example, in Fig. 5, suppose that the two $PU - TX$ s occupy channel m_1 and m_2 , and are randomly active. Route R that goes out from sector III of node c is different from route R' that goes from sector IV . Intuitively, when channel m_1 is unavailable, route R is better than route R' because the following links of c on route R' are more likely to be broken, which is unreliable and would cause more delay.

C. Threshold Based Piggyback Scheme with Limited Overhead

Having the boundary node definition, each node can identify if it is, itself, a boundary node of a certain primary user during the spectrum sensing phase. Our protocol will make use of boundary nodes during the piggyback phase.

As stated at the beginning of this section, when node a receives the RREQ packet, it will add both its ID and the 2-tuple (IN_a, OUT_a) to the RREQ. However, if a is a boundary node of the PU occupying channel m , and the active probability of that PU is above a predefined threshold γ , it will add the 4-tuple (IN_a, OUT_a, m, μ_a) to the RREQ, where μ_a equals 1 or -1, indicating the entrance to, or exiting of, the PU area. More specifically, we provide the following three cases for node a to decide which information it will add to the current RREQ packet:

- If $\exists m \in M$ that satisfies $B_a(m) = 1$ & $PB_a(m) > \gamma$, and m is unavailable on the sector number OUT_a from which the RREQ is sent out, rather than a 's ID and its 2-tuple (IN_a, OUT_a) , a would add the 4-tuple

(IN_a, OUT_a, m, μ_a) to the RREQ, where m is the channel that is unavailable in sector OUT_a , and $\mu_a = 1$, which indicates the entrance to the PU area.

- If $\exists m \in M$ that satisfies $B_a(m) = 1$ & $PB_a(m) > \gamma$, and m is unavailable on the sector number IN_a from which the RREQ is received, a would add its ID and the 4-tuple (IN_a, OUT_a, m, μ_a) to the RREQ, where m is the channel that is unavailable in sector IN_a , and $\mu_a = 0$, which indicates an exit from the PU area.
- Otherwise, a would only add its ID and the 2-tuple (IN_a, OUT_a) to the RREQ.

The first case presents the situation in which the route enters the PU area occupying m , reported by the boundary node a . The second case represents the situation in which the route leaves the PU area occupying m , reported by the boundary node a . In both cases, the PU occupying m does not have to be active at the time when RREQ is transmitted, as long as they are previously measured by the boundary nodes and their active probability measured by a is above a predefined threshold γ . The third case is for nodes that are not boundary nodes, or nodes that are boundary nodes but the active probability of PU is below the threshold γ , regardless of if they are inside or outside the PU areas.

The reason that the active probability of PU during T has to be above the predefined threshold γ is because different PUs have different active levels. For example, some PUs are much less frequently active than other PUs. It is possible that entering these PU areas could achieve a better performance than choosing other routes, which do not go through those PU areas but take longer hop distances to reach the destination. The route selection algorithm is discussed in details in the following parts.

For example, in Fig. 5, the two $PU - TX$ s occupy channels m_1 and m_2 . There are two optional routes, R and R' , from source S to destination D . Node j in Fig. 5 satisfies the first case, where $B_j(m_2) = 1$, and m_2 is unavailable on sector I ($OUT_j = I$). j would add its ID and the 4-tuple $(II, I, m_2, 1)$ to the RREQ. Node h in Fig. 5 belongs to the second case. Thus, h would add its ID and $(II, I, m_2, -1)$ to the RREQ. Node i in Fig. 5 meets the conditions of the third case. Therefore, i only adds its ID and (I, IV) to the RREQ.

After the destination node D is reached, it copies the route information and the added 2 or 4-tuple information by each node in RREQ, and piggybacks to source node S in RREP. Using route R in Fig. 5 as an example, the RREP would contain the node IDs, $\langle S, c, i, j, g, h, D \rangle$, on R , and also the 2 or 4-tuple attributes of each node. Among all nodes on route R , j has the 4-tuple $(II, I, m_2, 1)$, and h has the 4-tuple $(II, I, m_2, -1)$. The others have 2-tuple, indicating the IN and OUT sector numbers.

D. Weighted Route Length

After the source node receives the RREP along with piggybacked information, it needs to perform the route selection, since there is usually more than one route that can reach the destination node.

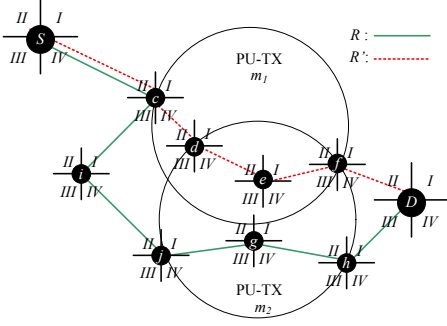


Fig. 5. Two possible routes from S to D .

Due to the dynamics of channel availabilities, it is impractical to estimate the delay of each route and choose the optimal one. To achieve our goal, we provide a heuristic approach to estimate the delay of each route. There are two factors to be considered: the delay of each link along the route, and the length of the route. The transmission rate depends on the power used by the sender. Based on the constraints in 3, the maximal power that a node can use happens when that channel is free of the corresponding PU area. Intuitively, the route that passes through the lower amount of PU area is more likely to achieve less delay for each link. Instead of adopting the traditional way to calculate the route length, we propose a novel weighted route length calculation, which connects the channel availabilities of each route with the route length.

The calculation of the route length is conducted by the source node, which makes use of the information contained in the piggybacked RREP packet. We use ab to denote a single link from a to b on the optional route. a and b have a 2-tuple or 4-tuple attribute, depending on whether it is a boundary node or not.

We start by defining whether a link is inside or outside a PU area that occupies channel m . The source node treats the nodes that return a 2-tuple as a non-boundary node. For example, as discussed in the above part, if a node a is a boundary node but the active probability of PU is below a threshold, it only returns a 2-tuple. The source node would treat a as a non-boundary node, as well as other real non-boundary nodes.

Definition 2: A single link ab is inside the PU area that occupies channel m if any of the three cases is satisfied:

- $B_a(m) = 1, \mu_a = 1$;
- $B_a(m) = 0, B_b(m) = 1, \mu_b = -1$;
- $B_a(m) = 0, B_b(m) = 0$, and $\exists c$, which satisfies $B_c(m) = 1$; c is the nearest boundary node to a among all the boundary nodes before a on the given route, and it satisfies $\mu_c = 1$.

Otherwise, the link is outside the PU area of m . For a given route, we use $I_{ab}(m) = 1$ to denote that the link ab is inside the PU area of m , and $I_{ab}(m) = 0$ to denote it is outside the PU area of m .

In the above definition, the first case means that node a is the starting point of entering the PU area occupying m . The second case means that node b is the end point of leaving

Algorithm 1 Route selection from route set \mathcal{R} .

1. $Length = \infty, Route = null$
 2. **for** $\forall R \in \mathcal{R}$ **do**
 3. Calculate $L(R)$ using (6) // Calculate the route length of every R
 4. **if** $L(R) < Len$ **then**
 5. $Route = R$
 6. $Length = L(R)$
 7. **end if**
 8. **end for**
 9. return $Route$ // Return the route with minimum length.
-

the PU area occupying m . The third case means that the link is inside the PU area, and neither of the two nodes is the boundary node. $B_a(m) = 0$ is necessary in the second case, which eliminates the case that $B_a(m) = 1, \mu_a = -1, B_b(m) = 1$, and $\mu_b = -1$, that is, both a and b denote leaving the same area. Links under this case should be considered to be outside the area of channel m . The source node S and the destination node D do not need to be considered, since they are not optional nodes on the route.

Next, we define the weighted length of a single link on a given route.

Definition 3: For a single link ab on a given route, the weighted length of the single link L_{ab} is calculated as:

$$L_{ab} = \begin{cases} 1 & I_{ab}(m) = 0, \forall m \in M; \\ \frac{|M|}{|M| - \mathcal{C}(m)} & I_{ab}(m) = 1; \end{cases} \quad (5)$$

where $\mathcal{C}(m)$ counts the number of channels on link ab that satisfy $I_{ab}(m) = 1$, which means ab is inside the PU area of m , and $|M|$ is the number of total channels in the network.

Therefore, we have the definition of the weighted length of a single route.

Definition 4: For a route R , the length of R is:

$$L(R) = \sum_{ab \in R} L(ab), \quad (6)$$

where ab is any link on the route R .

From the definition of the weighted route length, we can see that both the number of hops to reach the destination and the channel availabilities on the route are taken into consideration.

E. Route Selection Algorithm

For the source node S , after it receives the RREP from the destination node D , it will retrieve the information in the multiple RREP messages, and select one route to reach D . Suppose that the set of routes S can select from is \mathcal{R} . The algorithm for S to select a route from \mathcal{R} is in Algorithm 1. It will choose the route with the minimum weighted length, based on the definition in the previous part.

We use Fig. 5 as an example. Suppose there are 3 channels in total, which means $|M| = 3$. The weighted length values of each link on two optional routes, R and R' , are shown in Table I. Since $L(R) = 7$ and $L(R') = 19/2$, R is chosen as the route from S to D . The advantage of R can be seen when

TABLE I
EXAMPLE OF WEIGHTED ROUTE LENGTH

R	Sc	ci	ij	fg	gh	hD
7	1	1	1	$\frac{3}{2}$	$\frac{3}{2}$	1

R'	Sc	cd	de	ef	fD
$\frac{19}{2}$	1	$\frac{3}{2}$	3	3	1

TABLE II
SIMULATION SETTINGS

Number of nodes	[100, 300]
Number of channels	[10, 25]
Number of sectors	4
TX power	23 dBm
Noise power	-98 dBm
SINR threshold	10 dB
Number of PUs	[10, 50]
Operation range of each PU	[300, 500]
Delay for single channel switch	0.1 s

both PUs become active; links de and ef on R' only have one same channel available, making them unable to transmit simultaneously due to interference. Also, if another primary user suddenly joins this area, then R' is more likely to have broken links, which would cause more delay.

After the route is selected, each node on the selected route will sense the channels, and choose the one with maximum transmission rate, based on the constraints in (3).

F. Performance Analysis

We analyze the reliability increment of one link, on average, by comparing the route selected by our algorithm with the traditional shortest path.

Given a pair of source node S and destination node D , let N denote the node set of the route selected by our algorithm, and N_0 denote the node set of the shortest route selected by traditional greedy algorithm. Then we have:

$$N = N_0 + \Delta, \quad \Delta > 0, \quad (7)$$

where Δ is the difference in the number of nodes.

Theorem 1: We use \mathcal{Q} to denote the average number of PU areas that a single link on N is located inside, and \mathcal{Q}_0 for N_0 . Then

$$\frac{\mathcal{Q}_0}{\mathcal{Q}} > 1 + (\eta - 1) \frac{\Delta}{N}, \quad (8)$$

where $\mathcal{Q} = |M|/\eta$, $|M|$ is the total number of channels, and $\eta \geq 1$.

Proof: It is obvious that $|M| = \eta\mathcal{Q}$, and $\eta \geq 1$, since $|M|$ is the maximum possible number of channels that a single link can possibly be inside. From the definition in (6), and Algorithm 1, which ensures that the route consisting of \mathcal{N} has the minimum weighted length:

$$\begin{aligned} \frac{|M|}{|M| - \mathcal{Q}_0} \times N_0 &> \frac{|M|}{|M| - \mathcal{Q}} \times N \\ \frac{|M|}{|M| - \mathcal{Q}_0} \times N_0 &> \frac{|M|}{|M| - \mathcal{Q}} \times (N_0 + \Delta) \\ \frac{\mathcal{Q}_0}{\mathcal{Q}} &> \frac{N_0 + \frac{\Delta|M|}{\mathcal{Q}}}{N} \end{aligned}$$

Since $|M| = \eta\mathcal{Q}$,

$$\frac{\mathcal{Q}_0}{\mathcal{Q}} > \frac{N_0}{N} + \frac{\Delta\eta}{N}$$

Given $N = N_0 + \Delta$, then

$$\frac{\mathcal{Q}_0}{\mathcal{Q}} > 1 + (\eta - 1) \frac{\Delta}{N}. \quad \blacksquare$$

From Theorem 1, when PUs suddenly appears, the larger η will ensure a more reliable performance of Algorithm 1, compared to the traditional shortest path. This is because the larger $\mathcal{Q}_0/\mathcal{Q}$ provides a lower probability that a suddenly appearing PU will break a link on the route between S and D . A more reliable link reduces the delay, because the node of a broken link needs to perform handoff or rerouting to reach the next hop.

VI. PERFORMANCE EVALUATIONS

In this section, we perform simulations to evaluate the performance of our model. We first introduce the simulation settings. Then we present our simulation results.

A. Simulation Settings

We randomly distribute nodes in a $2,000 \times 2,000$ unit square. Each node has 4 sectors to send and receive data. We generate a number of PUs, which are randomly active on a certain channel. The operation range of each PU is different. The number of nodes is more than the number of PUs, and this ensures that the boundary of each PU is detected. We randomly choose a source and a destination. Then, using our approach, the source establishes a route to reach the destination. The channel availabilities are dynamic during the data transmission, because the PUs are set at a predefined probability to be active on a channel. The settings of our simulation parameters are shown in Table II. For simplicity, we set the channel switch delay to be constant.

The three parameters, the number of nodes, number of channels, and number of PUs, are tunable. We compare our model with the shortest path algorithm, which is to find the shortest path from the source to the destination, without considering the channel availabilities. We evaluate the performance of both models from the following aspects:

- Number of hops: simply count the number of links for each route, without considering other factors, e.g., the channel availabilities.
- Total delay: the overall delay considering both channel switching delay and data transmission delay of each session.
- Average route length: calculate the average route length in both models using Definition 4.

B. Simulation Results

We present our simulation results from the four aspects listed in the above portion.

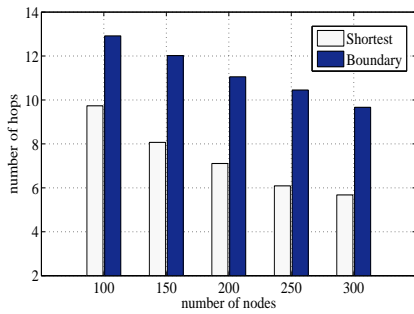


Fig. 6. Number of Hops

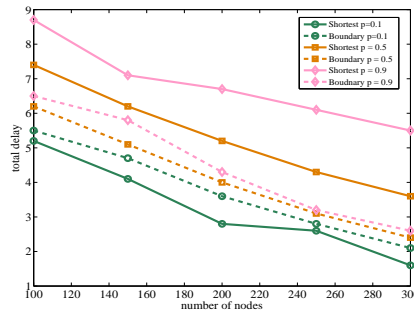


Fig. 7. Different Delay Comparisons

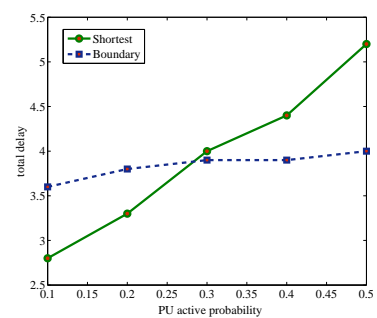


Fig. 8. PU Active Probabilities

1) *Number of hops*: we set the total number of PUs to 10, and the total number of channels to 10. The number of nodes varies from 100 to 300. We calculate the number of hops of each route under both models. The results are shown in Fig. 6. The line labeled as “Shortest” is the result from using the shortest path algorithm, without considering the channel availabilities. The line labeled as “Boundary” is the result from our model. Obviously, the shortest path algorithm has a lower number of hops than our algorithm. Moreover, in both models, the average number of hops reduces as the number of nodes increases. This is because the connectivity of the network increases when the number of nodes increases.

2) *Total delay*: we provide the comparison of the total delay for the routes of sessions under both models. We first evaluate the influence of different active PU probabilities on the delay. We set different PU active probabilities (0.1, 0.5, 0.9). We vary the number of nodes from 100 to 300 while keeping the number of channels as 10, and the number of PUs as 10. The results of total delay are shown in Fig. 7. We can tell that when the active probability equals 0.5 and 0.9, our boundary based algorithm is better than the shortest algorithm. When the PU active probability is 0.1, the shortest algorithm achieves shorter total delay than our model. Therefore, the larger the PU active probability is, the better performance our model will have, compared to the shortest algorithm.

From the above results, we know that the value of the PU active probability, where the two algorithms are close to each other, is between 0.1 and 0.5. Thus, we do more simulations to find the value by varying the active probability from 0.1 to 0.5. We keep the number of nodes as 200, the number of channels as 10, and the number of PUs as 10. The results are shown in Fig. 8. From Fig. 8, we can see that the total delay of the two algorithms are the closest when the PU active probability is between 0.25 and 0.3. Based on our threshold based piggyback scheme, we can set the threshold as 0.3 here. If the PU active probability is below 0.3, the boundary node does not need to piggyback its boundary information. In the following simulations, we set the PU active probability as 0.5.

We then study the influence of the three network parameters; the results are shown in Fig. 9. In Fig. 9(a), we vary the number of nodes from 100 to 300 while keeping the number of channels as 10, and the number of PUs as 10. The total

delay of both models decreases when the total number of nodes increases. Our model achieves about 1.0s less than the model using the shortest algorithm. Besides, in both models, as the number of nodes increases, the total delay increases more slowly. In Fig. 9(b), we vary the number of channels from 10 to 25, while keeping the number of nodes as 200, and the number of PUs as 10. The total delay of both models decreases as the total number of channels increases. Under this setting, our model achieves about 20% less total delay than those using the shortest algorithm. In Fig. 9(c), we vary the number of PUs while keeping the number of nodes as 200, and the number of channels as 10. The total delay of models increases when the total number of PUs increases. Our model achieves about 20% less total delay than those using the shortest algorithm. In addition, when the number of PUs increases, the total delay of the model using the shortest algorithm increases more quickly. Our model increases much more slowly compared to the shortest algorithm. Therefore, our model is more reliable when facing the more dynamic channel availabilities.

3) *Average route length*: we compare the average route length by varying the three tunable parameters: number of nodes, number of channels, and number of PUs, similar to the above settings. In Fig. 10(a), the average route length decreases in both models. This is because the number of hops in both models decreases when the number of nodes increases. The average route length in our model is about 40% less than the shortest path algorithm. In Fig. 10(b), the average route length decreases in both models. The average route length using the shortest algorithm is 30% more than in our model. Our model decreases more slightly because it is already close to the minimum value, which equals the number of hops. In Fig. 10(c), the average route length increases in both models when the number of PUs increases. This is because, when there are more PUs, more links are within the PU area. In addition, the average route length in our model is about 40% less than the shortest algorithm.

VII. CONCLUSION

In this paper, we propose an efficient model for routing in CRNs, which considers the dynamic channel availabilities. We assume that the directional antenna is equipped on each

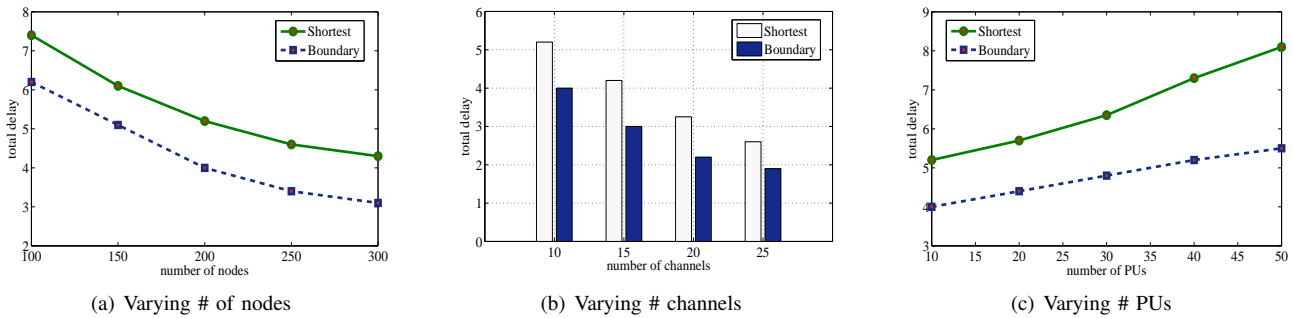


Fig. 9. Comparison of the total delay by varying network parameters.

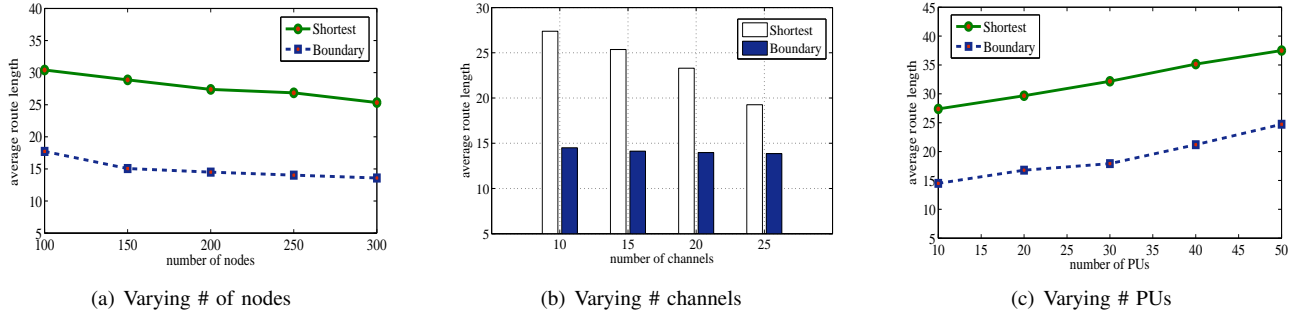


Fig. 10. Comparison of the average route length by varying network parameters.

node, aiding each node in determining whether it is a boundary node, and also creating more channel opportunities. Each boundary node is located at the boundary of a PU area. We use the USRP/Gnuradio testbed to prove the differences of the sensing results by boundary nodes in different directions. The boundary nodes help to estimate the channel situation of each optional route, and also the number of links located within a PU area on each route. Nodes on each route piggyback the channel availability and path information. In our model, the piggyback scheme is very efficient and only causes limited overhead. We give a novel definition of the route path, and propose an effective algorithm for route selection. We analyze the reliability of our algorithm. We perform numerous simulations to testify the performance of our model.

ACKNOWLEDGMENTS

This research was supported in part by NSF grants ECCS 1231461, ECCS 1128209, CNS 1138963, CNS 1065444, and CCF 1028167.

REFERENCES

- [1] I. F. Akyildiz, W.-Y. Lee, and K. R. Chowdhury, "CRAHNs: Cognitive radio ad hoc networks," *Ad Hoc Networks*, vol. 7, pp. 810–836, 2009.
- [2] M. Cesana, F. Cuomo, and E. Ekici, "Routing in cognitive radio networks: Challenges and solutions," *Ad Hoc Networks*, 2010.
- [3] R. Vilzmann and C. Bettstetter, "A survey on mac protocols for ad hoc networks with directional antennas," in *EUNICE 2005: Networks and Applications Towards a Ubiquitously Connected World*, 2006.
- [4] F. Dai and J. Wu, "Efficient broadcasting in ad hoc wireless networks using directional antennas," *IEEE Transactions on Parallel and Distributed Systems*, 2006.
- [5] Y. Liu, L. Cai, and X. Shen, "Spectrum-aware opportunistic routing in multi-hop cognitive radio networks," *IEEE Journal on Selected Areas in Communications*, 2012.

- [6] K. R. Chowdhury and I. F. Akyildiz, "CRP: A routing protocol for cognitive radio ad hoc networks," *IEEE Journal on Selected Areas in Communications*, 2011.
- [7] A. Raniwala, K. Gopalan, and T. Chiu, "Centralized channel assignment and routing algorithms for multi-channel wireless mesh networks," *ACM Mobile Computing and Communications*, 2004.
- [8] J. So and N. H. Vaidya, "Routing and channel assignment in multi-channel multi-hop wireless networks with single-nic devices," *Technical Report*, 2004.
- [9] H. Wu, F. Yang, K. Tan, J. Chen, Q. Zhang, and Z. Zhang, "Distributed channel assignment and routing in multi-radio multi-channel multi-hop wireless networks," *Technical Report*, 2006.
- [10] G. Zhao, J. Ma, G. Y. Li, T. Wu, Y. Kwon, A. Soong, and C. Yang, "Spatial spectrum holes for cognitive radio with relay-assisted directional transmission," *IEEE Transactions on Wireless Communications*, 2009.
- [11] D. Wilcox, E. Tsakalaki, A. Kortun, T. Ratnarajah, C. Papadias, and M. Sellathurai, "On spatial domain cognitive radio using single-radio parasitic antenna arrays," *IEEE Journal on Selected Areas in Communications*, 2013.
- [12] W. Guo and X. Huang, "Multicast communications in cognitive radio networks using directional antennas," *Wireless Communications and Mobile Computing*, 2012.
- [13] W. Guo, X. Huang, and K. Zhang, "Joint optimization of antenna orientation and spectrum allocation for cognitive radio networks," in *the Forty-Third Asilomar Conference on Signals, Systems and Computers*, 2009.
- [14] L. Cao, L. Yang, X. Zhou, Z. Zhang, and H. Zheng, "Optimus: SINR-driven spectrum distribution via constraint transformation," *Proc. of IEEE DySPAN*, 2010.
- [15] D. B. Johnson and D. A. Maltz, "Dynamic source routing in ad hoc wireless networks," *Kluwer Academic*, 1996.
- [16] J. T. Chiang, D. Kim, and Y.-C. Hu, "Jim-beam: Using spatial randomness to build jamming-resilient wireless flooding networks," in *Proc. of ACM Mobihoc*, 2012.
- [17] X. Zhou, R. Ganti, and J. Andrews, "Secure wireless network connectivity with multi-antenna transmission," *IEEE Transactions on Wireless Communications*, 2011.